

LETTERS

Unique features of action potential initiation in cortical neurons

Björn Naundorf^{1,2,3}, Fred Wolf^{1,2,3} & Maxim Volgushev^{4,5}

Neurons process and encode information by generating sequences of action potentials^{1,2}. For all spiking neurons, the encoding of single-neuron computations into sequences of spikes is biophysically determined by the cell's action-potential-generating mechanism. It has recently been discovered that apparently minor modifications of this mechanism can qualitatively change the nature of neuronal encoding^{3,4}. Here we quantitatively analyse the dynamics of action potential initiation in cortical neurons *in vivo*, *in vitro* and in computational models. Unexpectedly, key features of the initiation dynamics of cortical neuron action potentials—their rapid initiation and variable onset potential—are outside the range of behaviours described by the classical Hodgkin–Huxley theory. We propose a new model based on the cooperative activation of sodium channels that reproduces the observed dynamics of action potential initiation. This new model predicts that Hodgkin–Huxley-type dynamics of action potential initiation can be induced by artificially decreasing the effective density of sodium channels. *In vitro* experiments confirm this prediction, supporting the hypothesis that cooperative sodium channel activation underlies the dynamics of action potential initiation in cortical neurons.

We analysed action potentials elicited in cortical neurons *in vivo* and *in vitro*, either spontaneously or in response to various stimuli. In all cells examined and for all conditions tested, the dynamics of action potential initiation was characterized by a very abrupt onset and a steep upstroke in membrane potential. In membrane potential traces, the abrupt onset of action potentials is apparent as a sharp kink (Fig. 1a, c). This phenomenon stands out even more clearly in phase plots that graph the rate of change of the membrane potential dV/dt against the instantaneous membrane potential $V(t)$, and is manifested as an almost vertical take-off in dV/dt versus V trajectories at action potential onset (Fig. 1b, d). In phase plots, an action potential is represented by a loop. At the start of the loop, the velocity increases rapidly from less than 5 mV ms^{-1} to more than 20 mV ms^{-1} . This several-fold increase in velocity occurs within a range of less than 1 mV and takes less than 0.2 ms. This onset behaviour is not a peculiarity of neurons *in vivo*. Neurons *in vitro* show similarly fast dynamics of action potential initiation (Fig. 1c, d). These dynamic features of recorded action potential onsets distinguish them from the behaviour of previously proposed computational models. Figure 1e, f shows a simulated action potential using a recently developed conductance-based model of a cortical neuron⁵. In this model, a velocity of 20 mV ms^{-1} is only reached over a range of 7–8 mV after about 1 ms. Thus, the real onset of cortical action potentials is approximately ten times faster than predicted by the model.

The rapid onset of action potentials is a very robust phenomenon, apparent during spontaneous and evoked activity *in vivo*. Moreover,

it is independent of the temporal structure of synaptic inputs (Fig. 2) and of the electrophysiological cell class (Fig. 4). Fig. 2 shows phase plots and membrane potential traces from a simple cell (Fig. 2a, b) and a complex cell (Fig. 2c, d) recorded *in vivo* in cat visual cortex. In the phase plots, subthreshold membrane potential fluctuations are represented by a grey cloud. In both the simple and the complex cell, action potentials rise almost vertically out of this cloud. Detecting the point at which the rate of change reaches a value of 10 mV ms^{-1} thus allows reliable identification of the time of action potential initiation

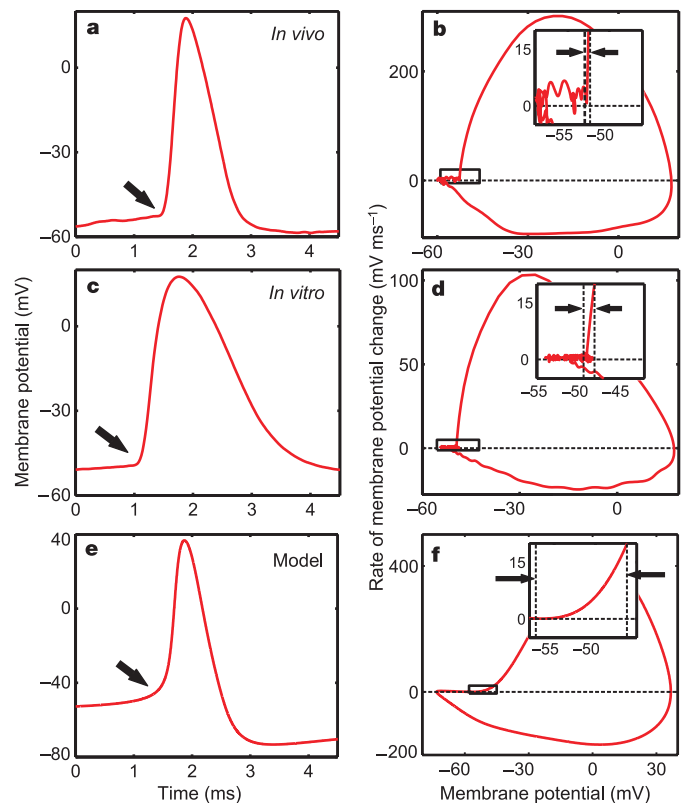


Figure 1 | Dynamics of action potential initiation in neocortical neurons and in a Hodgkin–Huxley-type model of a neocortical neuron. **a**, Action potential in a cat visual cortex neuron *in vivo*. The arrow shows the characteristic kink at action potential onset. **b**, Phase plot (dV/dt versus V) of the action potential from **a**. Inset shows the initial phase of the action potential. **c**, **d**, Action potential from a cat visual cortex slice *in vitro* at 20°C . **e**, **f**, Action potential from a Hodgkin–Huxley-type model of a neocortical neuron⁵.

¹Max Planck Institute for Dynamics and Self-Organization, ²Department of Physics and ³Bernstein Center for Computational Neuroscience, University of Göttingen, Bunsenstr. 10, D-37073 Göttingen, Germany. ⁴Department of Neurophysiology, Ruhr-University Bochum, D-44780 Bochum, Germany. ⁵Institute of Higher Nervous Activity and Neurophysiology Russian Academy of Sciences, Moscow 117485, Russia.

and the onset potential. The phase plots also show a second salient feature of cortical action potentials: the onset potentials vary considerably, over ranges of up to 10 mV (Fig. 2a–d) (Special care was taken to exclude any non-stationarities, see Supplementary Information). This distinct variability in onset potentials has previously been observed in cat visual cortex^{6–8} and rat hippocampus⁹. This second feature of cortical action potentials is also missing in Hodgkin–Huxley-type models. Figure 2e, f depicts the behaviour of such a model driven by fluctuating synaptic inputs⁵. The variability in onset potentials in this model is restricted to a range of less than 2 mV, which is much smaller than observed *in vivo*.

Two features thus render cortical action potentials distinctly different from simulated action potentials using Hodgkin–Huxley-type models. First, the initial action potential phase is approximately ten times faster in recorded neurons compared to conductance-based models. Second, the onset potential variability is approximately five times larger in the recorded cells. We tried, using various modifications of the models, to achieve a better match between recorded and simulated action potentials (including and/or modifying adaptation currents¹⁰, channel stochasticity¹¹, state-dependent inactivation¹², sodium channel activation curves and peak conductances; see Supplementary Information). None of the modified models reproduced the two salient features of the recorded action potentials.

In fact, a straightforward analysis reveals that rapid action potential onset and large variability in onset potentials are strongly antagonistic in Hodgkin–Huxley-type models. In such models, the initial phase of an action potential is determined by the activation of

voltage-dependent sodium channels. Their dynamics is described by the activation curve and kinetics of an associated gating variable. In the Hodgkin–Huxley formulation it can be shown that the rate of membrane depolarization is limited by $g_{\text{Na}}h_0m_{\infty}^3(V)(V_{\text{Na}} - V)/C + I_0/C$, where g_{Na} denotes peak sodium conductance, h_0 is the fraction of sodium channels available for activation, $m_{\infty}^3(V)$ is their activation curve, V_{Na} is the sodium reversal potential, C the membrane capacitance, and I_0 is the current carried by other channels. This upper bound on the rate of membrane potential change links the action potential onset dynamics directly to the width of the activation curve and peak sodium conductance. Figure 3 illustrates this relationship. An experimentally obtained activation curve from patches of cortical neurons^{13,14} results in a shallow action potential onset (Fig. 3a, b). Increasing the steepness of the activation curve leads to sharper action potential onsets, but even with a fivefold increase, the simulated action potentials do not rise as fast as those recorded. Changing the effective peak sodium conductance—mimicking inactivation^{6,9}—leaves the steepness of action potential onset unaffected but shifts the onset potentials (Fig. 3c, d). At the same time, increasing the steepness of the activation curve considerably decreases onset potential variability (Fig. 3e–f). Quantitatively, the variability of onset potentials is restricted by $\Delta V \approx k \log G$, where k is the width of the activation curve and G is the ratio of maximum to minimum peak conductance (see Supplementary Information). To mimic the measured combinations of onset rapidness and variability, unphysiologically large values of G (about 20,000) would be required.

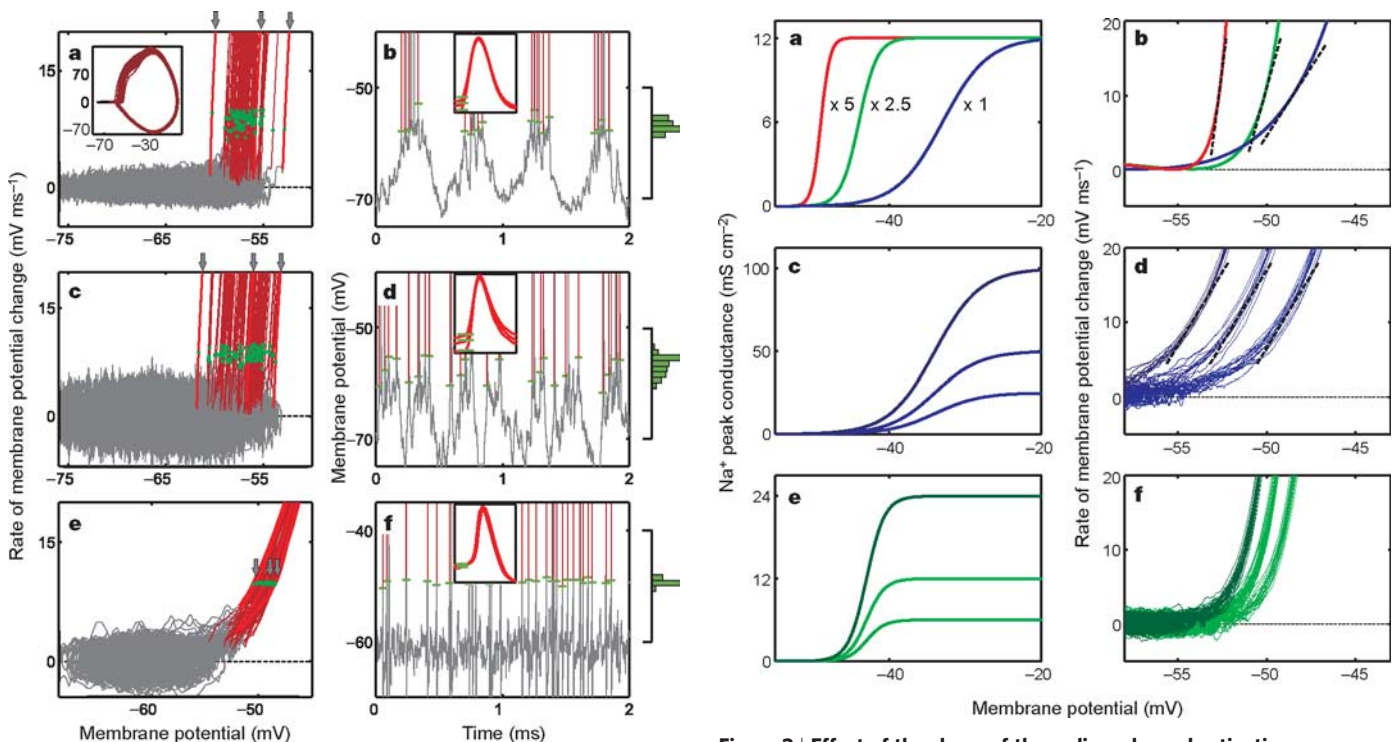


Figure 2 | Different action potential initiation in visual cortex neurons recorded *in vivo* and in a Hodgkin–Huxley-type model subject to fluctuating synaptic inputs. **a**, Phase plot of a simple cell response to a moving grating of optimal orientation. Subthreshold fluctuations are shown in grey, action potentials in red, and green dots indicate action potential onsets. The inset shows the complete trace. Arrows indicate three sample action potentials. **b**, Part of the recording from **a**, using the same colour code, with action potentials truncated in amplitude. Green bars show action potential onset potentials. Inset shows the action potentials marked with arrows in **a**. The histogram to the right shows the distribution of action potential onset potentials. **c**, **d**, Response of a complex cell. **e**, **f**, Response of a Hodgkin–Huxley-type model⁵ subject to fluctuating synaptic input.

Figure 3 | Effect of the shape of the sodium channel activation curve and effective peak conductance on action potential initiation in a Hodgkin–Huxley-type model. Activation curves used in the model (**a**, **c**, **e**) and initial phases of resulting action potentials (**b**, **d**, **f**) are shown using matched colours. Blue lines show standard activation curves¹⁴. **a**, **b**, Increasing the steepness of the activation curve (**a**) leads to a more rapid action potential upstroke (**b**). Dashed lines indicate tangents at 10 mV ms⁻¹. **c**–**f**, Initiation of action potentials with shallow (**c**, **d**) and steep (**e**, **f**) activation curves and different sodium peak conductances in a model driven by fluctuating synaptic inputs (several action potentials superimposed). Changing peak conductance shifts the action potential onset potential but does not affect its onset rapidness. Steeper activation curves lead to smaller action potential onset spans (**d**, 6 mV; **f**, 2.5 mV).

To quantitatively compare the action potential onset dynamics in our recordings with action potential dynamics in Hodgkin–Huxley-type models, we plotted the action potential onset span (difference between maximum and minimum onset potential in a recording) against the rapidness of action potential onset (the slope of the phase plot at $dV/dt = 10 \text{ mV ms}^{-1}$) for real and simulated recordings (Fig. 4). In the simulations, we used two different models^{5,10} driven by fluctuating synaptic currents. In both models we systematically changed the peak sodium conductance and the activation curve over the entire range in which action potentials were generated. The locations of data points from the model simulations reflect the antagonism between onset span and rapidness. Simulated action potentials either showed a large onset rapidness or a large onset span, but never both. The points representing simulated action potentials are clearly separated from the points representing *in vivo* action potentials, which show rapid onset dynamics and large variability in onset potentials, irrespective of the electrophysiological cell type. Action potentials recorded *in vitro* had similarly fast onset dynamics (Fig. 4).

The above arguments and our extensive simulations indicate that the dynamics of action potential initiation in cortical neurons deviates qualitatively from the classical picture described by the Hodgkin–Huxley framework. What could be the biophysical mechanism that enables cortical action potentials to initiate much faster and at the same time with a much larger onset potential variability than predicted by the Hodgkin–Huxley theory? According to this theory, there is a one-to-one relationship between the single-channel activation curve and the action potential onset dynamics, owing to the assumption that the opening of individual sodium channels is statistically independent. This assumption, however, might be violated in the highly organized molecular machinery of a living

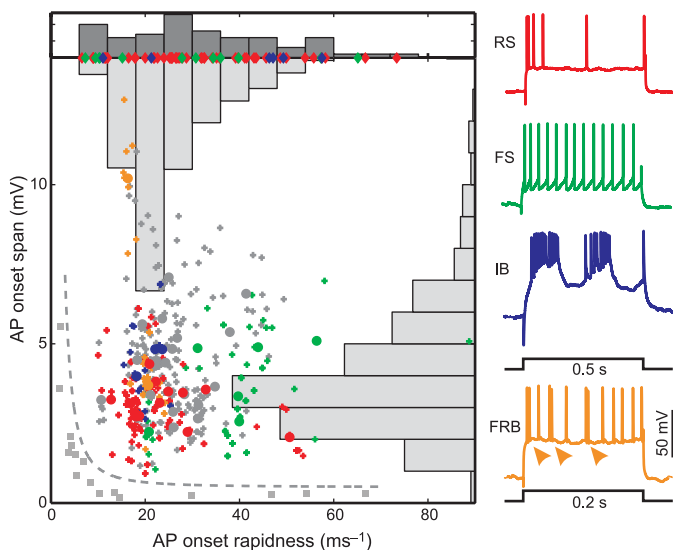


Figure 4 | Action potential onset span and rapidness in cortical neurons and Hodgkin–Huxley-type models. Points show data from cat visual cortex neurons *in vivo*, classified electrophysiologically as regular spiking (RS), fast spiking (FS), intrinsically bursting (IB) or fast rhythmic bursting (FRB). Colours match the neuronal responses to current steps shown on the right. Grey points indicate electrophysiologically unidentified cells. Circles show the mean of several measurements for each cell (individual measurements indicated with crosses). Diamonds at the top of the panel show *in vitro* data (cat visual cortex in blue, rat visual cortex in red, mouse hippocampus in green). Grey squares show simulation results from two Hodgkin–Huxley-type models with varied sodium channel activation curves and peak conductances, driven by fluctuating synaptic inputs. Dashed grey line separates the model from experimentally derived data. Histograms show the marginal distributions of the *in vivo* (light grey bars) and *in vitro* (dark grey bars) data.

cell. Indeed, the rapid onset of action potentials suggests that many sodium channels open virtually simultaneously, that is, in a potentially cooperative fashion.

To assess whether cooperative activation of voltage-gated sodium channels can account for the two characteristic features of cortical action potential initiation, we constructed a model of a population of coupled sodium channels. In this model, the gating of individual sodium channels follows a scheme introduced by Aldrich, Corey, and Stevens¹⁵. It incorporates state-dependent inactivation from the open state and voltage-dependent inactivation from closed states^{15,16}. The key feature of our model is a coupling between neighbouring channels: the opening of a channel shifts the activation curve of each channel to which it is coupled towards more hyperpolarized values, thus increasing its probability of opening.

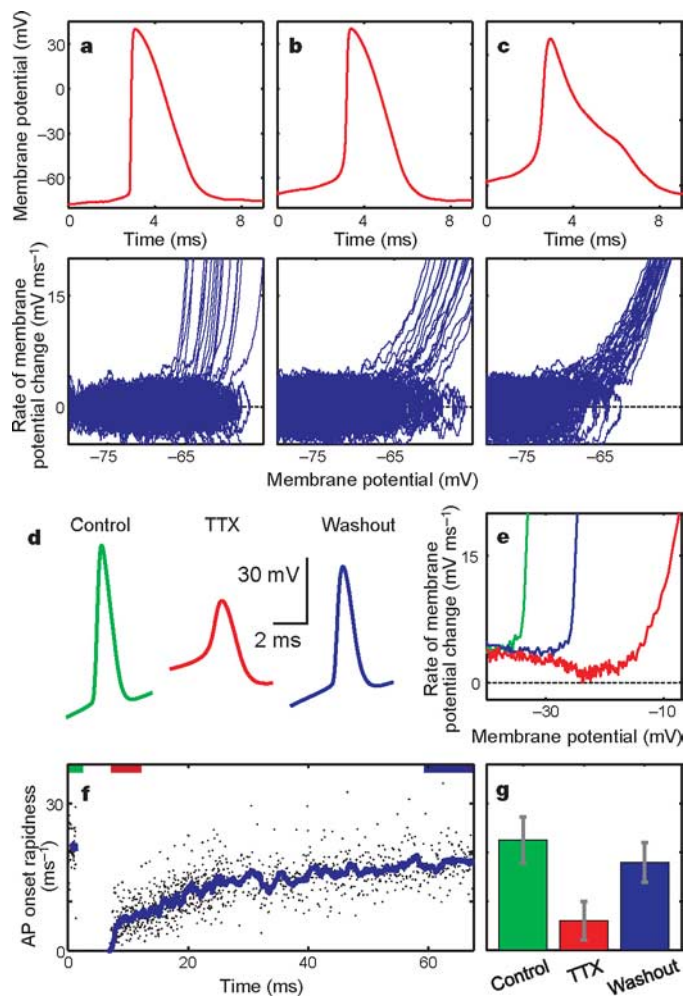


Figure 5 | Cooperative activation of voltage-gated sodium channels can account for the dynamics of action potential initiation in cortical neurons. **a**, Waveform (top) and phase plot (bottom) of action potentials elicited by fluctuating inputs in a conductance-based model that incorporates cooperative activation of sodium channels and closed-state inactivation. Both the action potential onset potential variability and onset rapidness are comparable to the *in vivo* recordings in Fig. 2. **b**, **c**, Same model, but without inter-channel coupling (**b**), and with Hodgkin–Huxley-like channel activation (**c**). **d–g**, Reducing the effective density of available sodium channels through TTX application reversibly reduces action potential amplitude and onset rapidness in cortical neurons *in vitro*. Shown are action potential waveforms (**d**) and phase plots of their initial parts (**e**). **f**, Time course of action potential onset rapidness in a cortical neuron before, during and after TTX application. **g**, Reversible reduction in onset rapidness of action potentials by TTX in six neurons. Error bars indicate s.e.m.

This model is able to reproduce the key features of cortical action potential initiation (Fig. 5a–c). With strongly cooperative activation, voltage-dependent inactivation from closed states, and slow de-inactivation (recovery from inactivation) of sodium channels, the simulated action potentials show both a large onset rapidness and large variability in onset potentials (Fig. 5a). Turning off the inter-channel coupling made the onset dynamics much shallower, while leaving onset variability unaffected (Fig. 5b). Hodgkin–Huxley-type dynamics of action potential onset was recovered when inactivation and de-inactivation were set to be fast and voltage-independent (Fig. 5c).

Assuming that channel interactions are distance-dependent in neuronal membranes, our model predicts that reducing the effective density of channels should weaken cooperativity, reduce the action potential onset rapidness and eventually lead to Hodgkin–Huxley-type onset dynamics. We tested this prediction *in vitro*, recording action potentials while reducing the density of available sodium channels by the application of tetrodotoxin (TTX). As expected, TTX application led to a decrease in action potential amplitude (Fig. 5d). More importantly, it also led to a substantial reduction in the onset rapidness of action potentials (Fig. 5d, e) in all tested cortical neurons (Fig. 5g), as predicted by our model. Moreover, gradual recovery of the number of available sodium channels during washout of TTX led to a gradual increase in action potential onset rapidness (Fig. 5f). These results cannot be explained by Hodgkin–Huxley-type models, in which reduction in the sodium channel density modifies only the amplitude of action potentials and their onset potential, but not their onset rapidness (see Fig. 3). Thus, in our opinion the fact that the dynamics of action potential initiation deviates qualitatively from voltage-dependent single channel activation points towards the cooperative activation of voltage-gated sodium channels.

Although our results are unexpected from a biophysical perspective, the combination of rapid dynamics and variable onset potentials of action potentials is beneficial for the coding of fast signals^{3,4} (see also Supplementary Information). With Hodgkin–Huxley-type dynamics of action potential initiation, the encoding of signals that vary on a timescale of less than 10 ms requires unphysiologically high mean firing rates that are likely to be energetically prohibitive^{17,18}. With action potential onset dynamics as described here for cortical neurons, much lower mean firing rates can support the encoding of such rapidly varying signals.

METHODS

In vivo and in vitro experiments. *In vivo* intracellular recordings were made using sharp electrodes in adult cats (3.0–4.5 kg). Data from 47 cells were used for the analysis. In each cell, we recorded responses to the presentation of moving gratings of different orientations (duration 5–7 s), and periods of spontaneous activity (10–120 s). Cells were classified functionally as either simple or complex using the spike response modulation index, and electrophysiologically by their responses to depolarizing current steps. *In vitro*, whole-cell recordings were made with patch electrodes in slices of rat or cat visual cortex and rat or mouse hippocampus. Data from 17 rat, 3 mouse and 2 cat neurons were analysed.

Computational models. We used two conductance-based Hodgkin–Huxley-type models^{5,10}, constructed to match the subthreshold membrane potential dynamics and firing statistics of cortical neurons. We introduced modifications to the models and varied model parameters over wide ranges in an attempt to reproduce the experimentally observed dynamics of action potential initiation. Action potential initiation by cooperative sodium channel activation was modelled using an effective mean field dynamics for a population of interacting sodium channels.

Details of experimental procedures and data analysis, and definitions of the models, their modifications and parameter ranges are provided in the Supplementary Information.

Received 22 October 2005; accepted 27 January 2006.

- Bernstein, J. Ueber den zeitlichen Verlauf der negativen Schwankung des Nervenstroms. *Pflügers Arch.* **1**, 173–207 (1868).
- Huxley, A. F. *Nobel Lectures, Physiology or Medicine 1963–1970* (Elsevier, Amsterdam, 1972).
- Fourcaud-Trocme, N., Hansel, D., van Vreeswijk, C. & Brunel, N. How spike generation mechanisms determine the neuronal response to fluctuating inputs. *J. Neurosci.* **23**, 11628–11640 (2003).
- Naundorf, B., Geisel, T. & Wolf, F. Action potential onset dynamics and the response speed of neuronal populations. *J. Comput. Neurosci.* **18**, 297–309 (2005).
- Destexhe, A. & Paré, D. Impact of network activity on the integrative properties of neocortical pyramidal neurons *in vivo*. *J. Neurophysiol.* **81**, 1531–1547 (1999).
- Azouz, R. & Gray, C. M. Dynamic spike threshold reveals a mechanism for synaptic coincidence detection in cortical neurons *in vivo*. *Proc. Natl Acad. Sci. USA* **97**, 8110–8115 (2000).
- Volgushev, M., Pernberg, J. & Eysel, U. T. A novel mechanism of response selectivity of neurons in cat visual cortex. *J. Physiol. (Lond.)* **540**, 307–320 (2002).
- Azouz, R. & Gray, C. M. Adaptive coincidence detection and dynamic gain control in visual cortical neurons *in vivo*. *Neuron* **37**, 513–532 (2003).
- Henze, D. A. & Buzsáki, G. Action potential threshold of hippocampal pyramidal cells *in vivo* is increased by recent spiking activity. *Neuroscience* **105**, 121–130 (2001).
- Wang, X. J., Liu, Y., Sanchez-Vives, M. V. & McCormick, D. A. Adaptation and temporal decorrelation by single neurons in the primary visual cortex. *J. Neurophysiol.* **89**, 3279–3293 (2003).
- Schneidman, E., Freedman, B. & Segev, I. Ion channel stochasticity may be critical in determining the reliability and precision of spike timing. *Neural Comput.* **10**, 1679–1703 (1998).
- Patlak, J. Molecular kinetics of voltage-dependent Na⁺ channels. *Physiol. Rev.* **71**, 1047–1080 (1991).
- Huguenard, J. R., Hamill, O. P. & Prince, D. A. Developmental changes in Na⁺ conductances in rat neocortical neurons: appearance of a slowly inactivating component. *J. Neurophysiol.* **59**, 778–795 (1988).
- Colbert, C. M. & Pan, E. Ion channel properties underlying axonal action potential initiation in pyramidal neurons. *Nature Neurosci.* **5**, 533–538 (2002).
- Aldrich, R. W., Corey, D. P. & Stevens, C. F. A reinterpretation of mammalian sodium channel gating based on single channel recording. *Nature* **306**, 436–441 (1983).
- Goldman, L. Stationarity of sodium channel gating kinetics in excised patches from neuroblastoma N1E 115. *Biophys. J.* **69**, 2364–2368 (1995).
- Attwell, D. & Laughlin, S. B. An energy budget for signaling in the grey matter of the brain. *J. Cereb. Blood Flow Metab.* **21**, 1133–1145 (2001).
- Lennie, P. The cost of cortical computation. *Curr. Biol.* **13**, 493–497 (2003).

Supplementary Information is linked to the online version of the paper at www.nature.com/nature.

Acknowledgements We would like to thank A. Borst, M. Brecht, M. Chistiakova, T. Geisel, T. Kottos, T. Moser, E. Neher, W. Stühmer, I. Timofeev and C. van Vreeswijk for discussions, A. Borst, M. Brecht and E. Neher for comments on earlier versions of the manuscript, and A. Malyshev for help in some of the experiments. This study was supported by grants from the Deutsche Forschungsgemeinschaft to M.V., by grants from the Human Frontier Science Program and the Bundesministerium für Bildung und Forschung to F.W., and by the Max-Planck Society.

Author Contributions B.N., F.W. and M.V. contributed equally to this work. All authors discussed the results and commented on the manuscript.

Author Information Reprints and permissions information is available at npg.nature.com/reprintsandpermissions. The authors declare no competing financial interests. Correspondence and requests for materials should be addressed to F.W. (fred@chaos.gwdg.de).

Copyright of Nature is the property of Nature Publishing Group and its content may not be copied or emailed to multiple sites or posted to a listserv without the copyright holder's express written permission. However, users may print, download, or email articles for individual use.